nature portfolio

https://doi.org/10.1038/s41596-021-00574-6

Supplementary information

Regional and functional division of functional elements of solid-state nanochannels for enhanced sensitivity and specificity of biosensing in complex matrices

In the format provided by the authors and unedited

Supplementary Information

Regional and functional division of functional elements of Solid-State Nanochannels for Enhanced Sensitivity and Specificity of Biosensing in Complex Matrices

Pengcheng Gao[1], Dagui Wang[1], Cheng Che[1], Qun Ma[1], Xiaoqing Wu[1], Yajie Chen[1], Hongquan Xu[1], Xinchun Li[2], Yu Lin[1], Defang Ding[1], Xiaoding Lou[1], Fan Xia[1], *

1 Engineering Research Center of Nano-Geomaterials of Ministry of Education, Faculty of Materials Science and Chemistry, China University of Geosciences (CUG), 388 lumo Road, Wuhan 430074, R. P. China.

2 Pharmaceutical Analysis Division, School of Pharmacy, Guangxi Medical University, 22 Shuangyong Road, Nanning 530021, P. R. China

*Corresponding authors: F. Xia, Tel.: (+86)-27-67885201. E-mail: xiafan@hust.edu.cn and xiafan@cug.edu.cn

Supplementary Figure 1

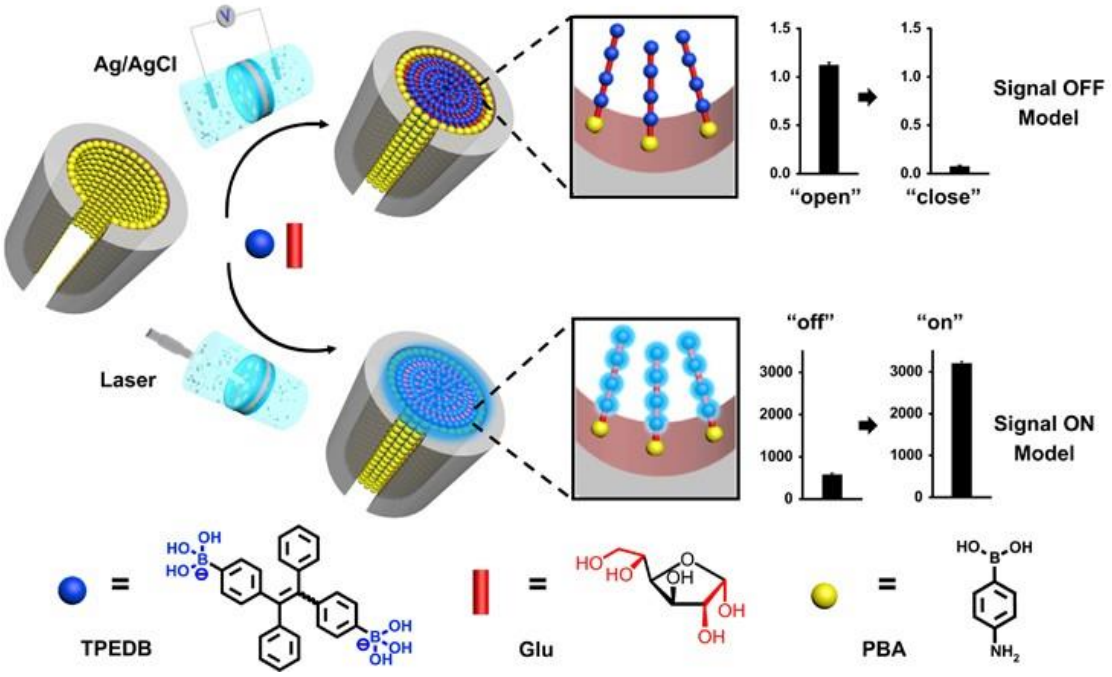

Supplementary Figure 1| Dual-signal-output nanochannels for glucose sensing. Scheme shows the sensing process. 4-aminophenylboronic acid (PBA) is used as capture probe and attached at the inner wall of the nanochannels. In presence of AIEgen (TPEDB, an aggregation-induced emission (AIE) molecule), the glucose molecules are captured at the PBA through the oligomerization reaction with TPEDB. The oligomer of the TPEDB and the glucose produces steric hindrance and decreases the ionic current through nanochannels (signal-off state). When TPEDB binds with glucose, the intramolecular motions of TPEDB are restricted, leading to the fluorescence emission. In LSCM, the binding of the TPEDB and the glucose activates the fluorescence and induces the fluorescent signal from off to on. Reprinted with permission from ref. S1, Nature Press.

Supplementary Figure 2

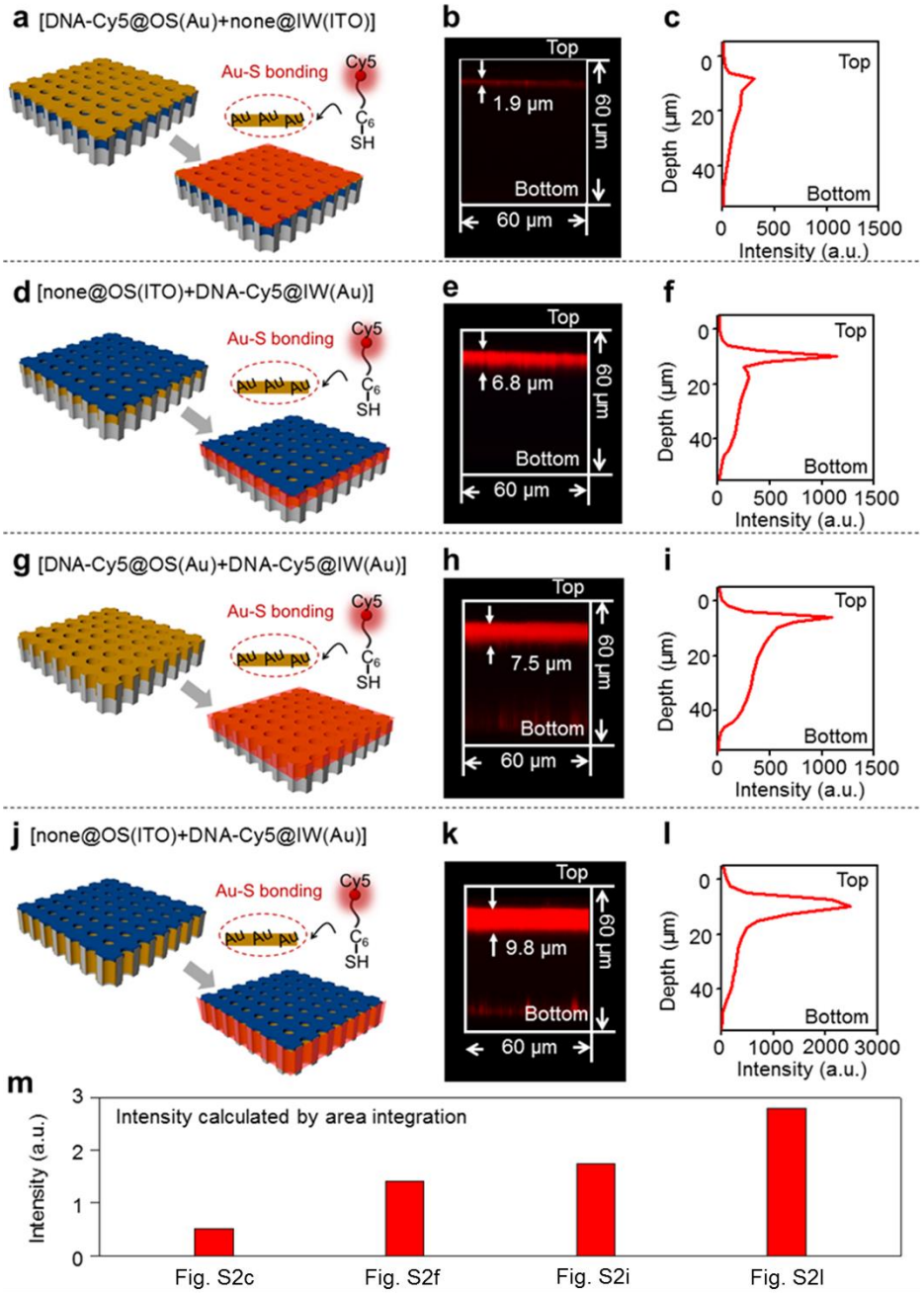

Supplementary Figure 2| LSCM image of DNA-Cy5 (3' end modified with -SH) modified metallic deposited nanochannels (Figure 2) from sectional view. Simple DNA-Cy5 (-SH modified at the 3' end) is added in the metallic deposited membranes. (a, b, c) [DNA-Cy5@OS(Au)+ none@IW(ITO)], (d, e, f) [none@OS(ITO)+DNA-Cy5@IW(Au)], (g, h, i) [DNA-Cy5@OS(Au)+DNA-Cy5@IW(Au)] and (j, k, l) [none@OS(ITO)+DNA-Cy5@IW (Au)]. (m) The integrated intensity of DNA-Cy5 along nanochannels calculated from the LSCM data (in Supplementary Figure 2c, f, i, l). reprinted with permission from ref. S2, Nature Press.

Supplementary Figure 3

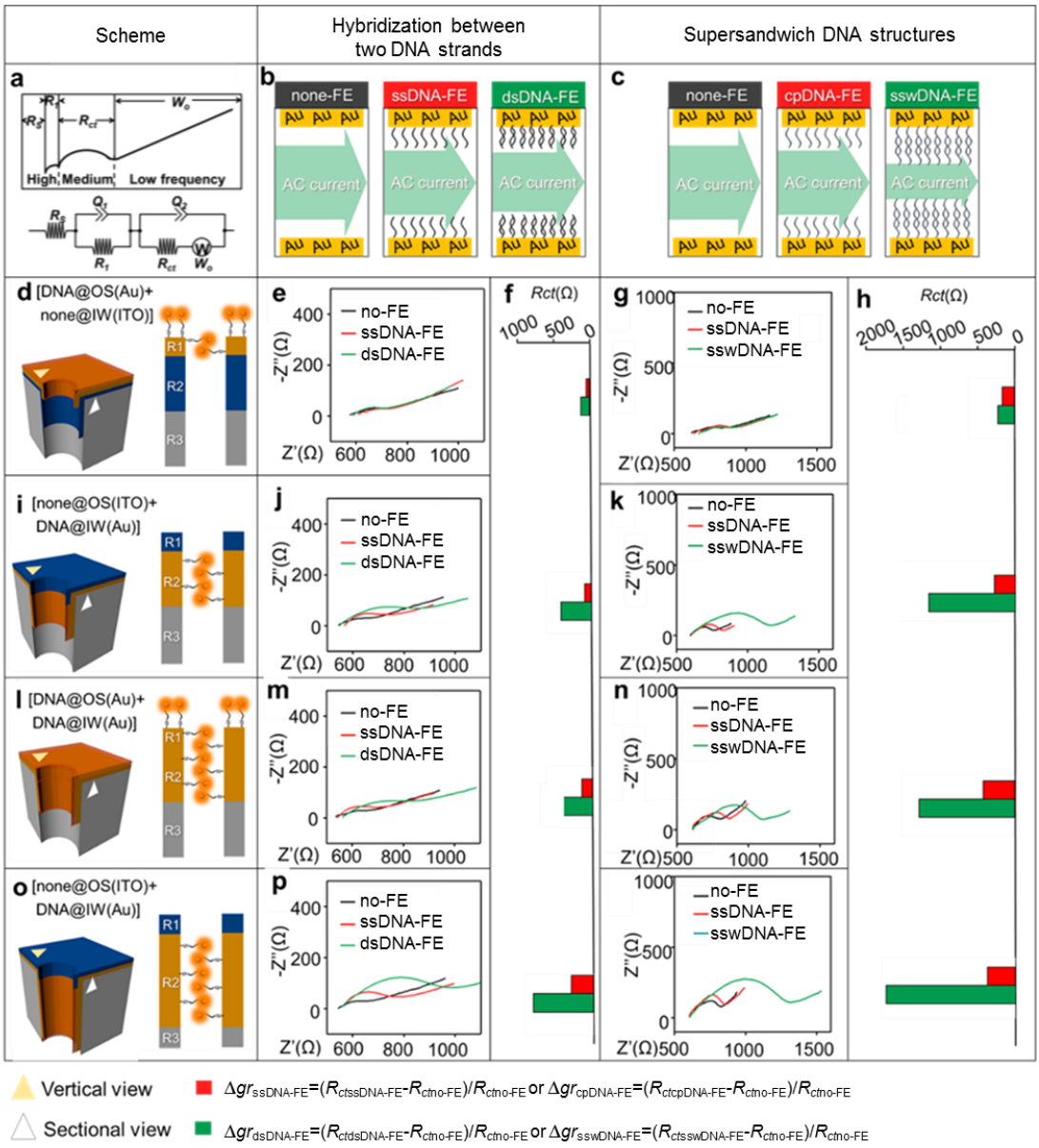

Supplementary Figure 3| EIS tests characterizing the resistance variation before and after DNA hybridization in Step20 (B). (a) EIS sketch and equivalent circuit used in the EIS tests. (b and c) scheme of AC current through nanochannels (d, i, l and o) Scheme reflecting the location of DNA and corresponding hybridization taking place. (e, j, m, p and f) the EIS sketch characterization the resistance variation of the DNA hybridization between probeDNA-SH and targetDNA. (g, k, n, q and h) the EIS sketch characterization the resistance variation of the formation of the DNA "supersandwich" nanostructure (ssw-DNA) consisted of cpDNA, SP1 and SP2. Reprinted with permission from ref. S2, Nature Press.

Supplementary Figure 4

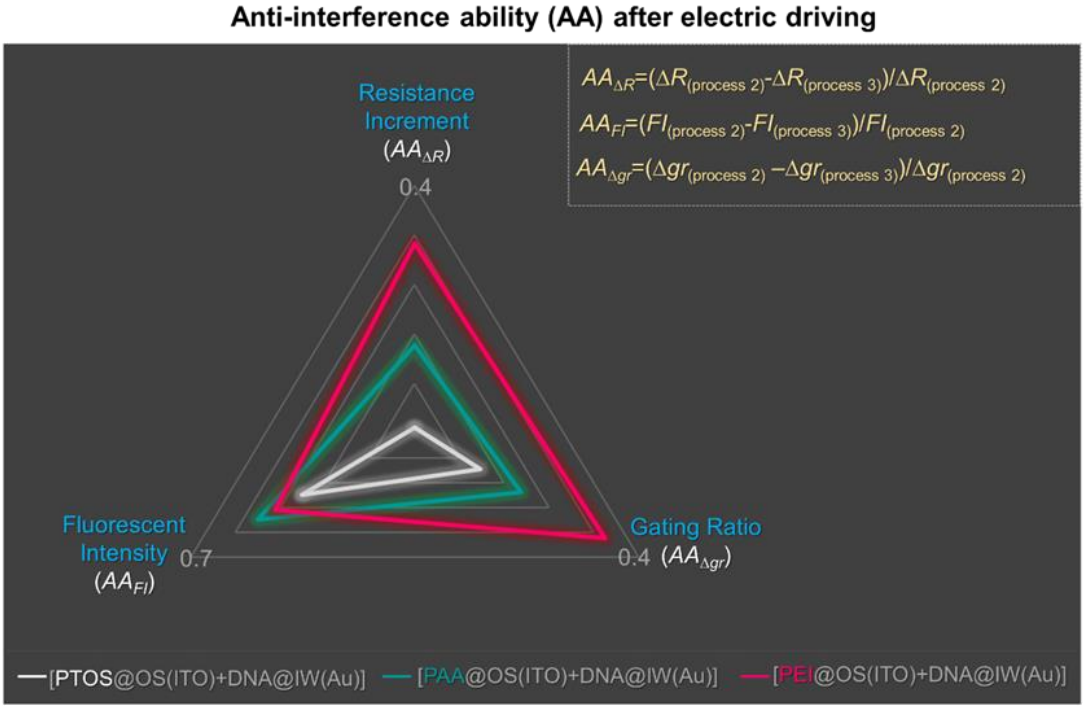

Supplementary Figure 4| The radar map integrated the three parameters reflecting the variation by the interference of ccDNA-Cy5 or AIEgens after 2 V driving. The three parameters are considered as the resistance variation before and after adding interference solution: d (AAΔR), gating ratio (AAΔgr), fluorescent intensity (AAFI). The calculated formulas are listed as AAΔR = (ΔR(process 2)-ΔR(process 3))/ΔR(process 2), AAFI=(FI(process 2)-FI(process 3))/FI(process 2), AAΔgr=(Δgr(process 2) – Δgr(process 3))/ Δgr(process 2) (where the Δgr are calculated by taking RBlank as 100 %). The bigger area of the polygon, the greater anti-interference of FEOS. Reprinted with permission from ref. S2, Nature Press.

Supplementary Figure 5

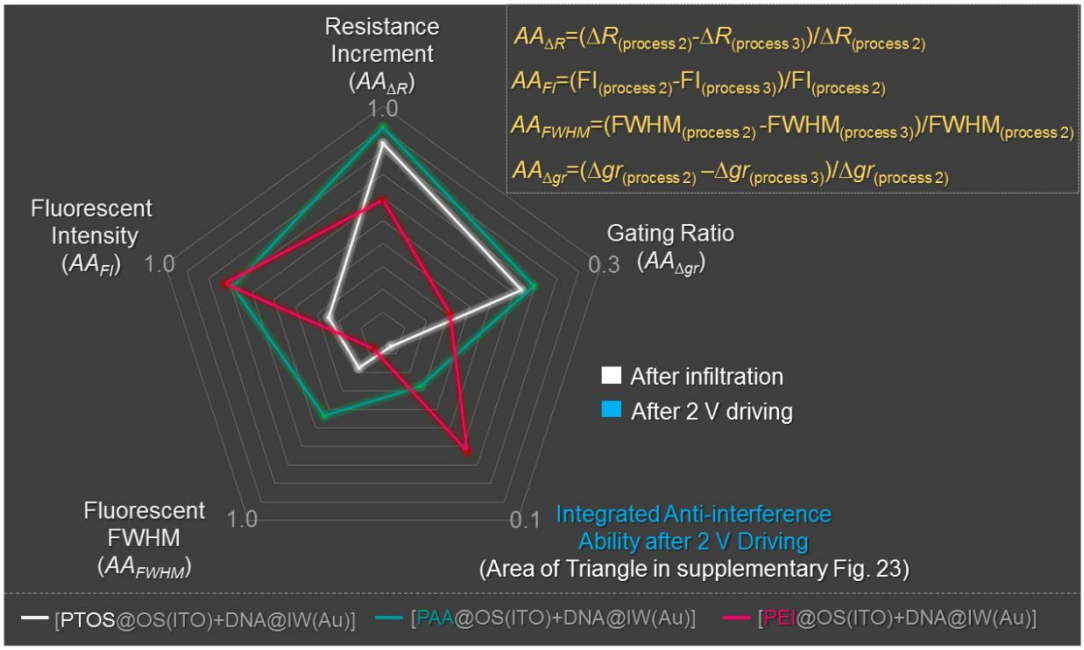

Supplementary Figure 5| Radar map describes the anti-interference ability of FEOS. A map consisted of five factors reflecting the variation after adding the interference through infiltration or 2 V driving. The greater area of the polygon, the better anti-interference ability of FEOS. Reprinted with permission from ref. S2, Nature Press.

Supplementary Figure 6

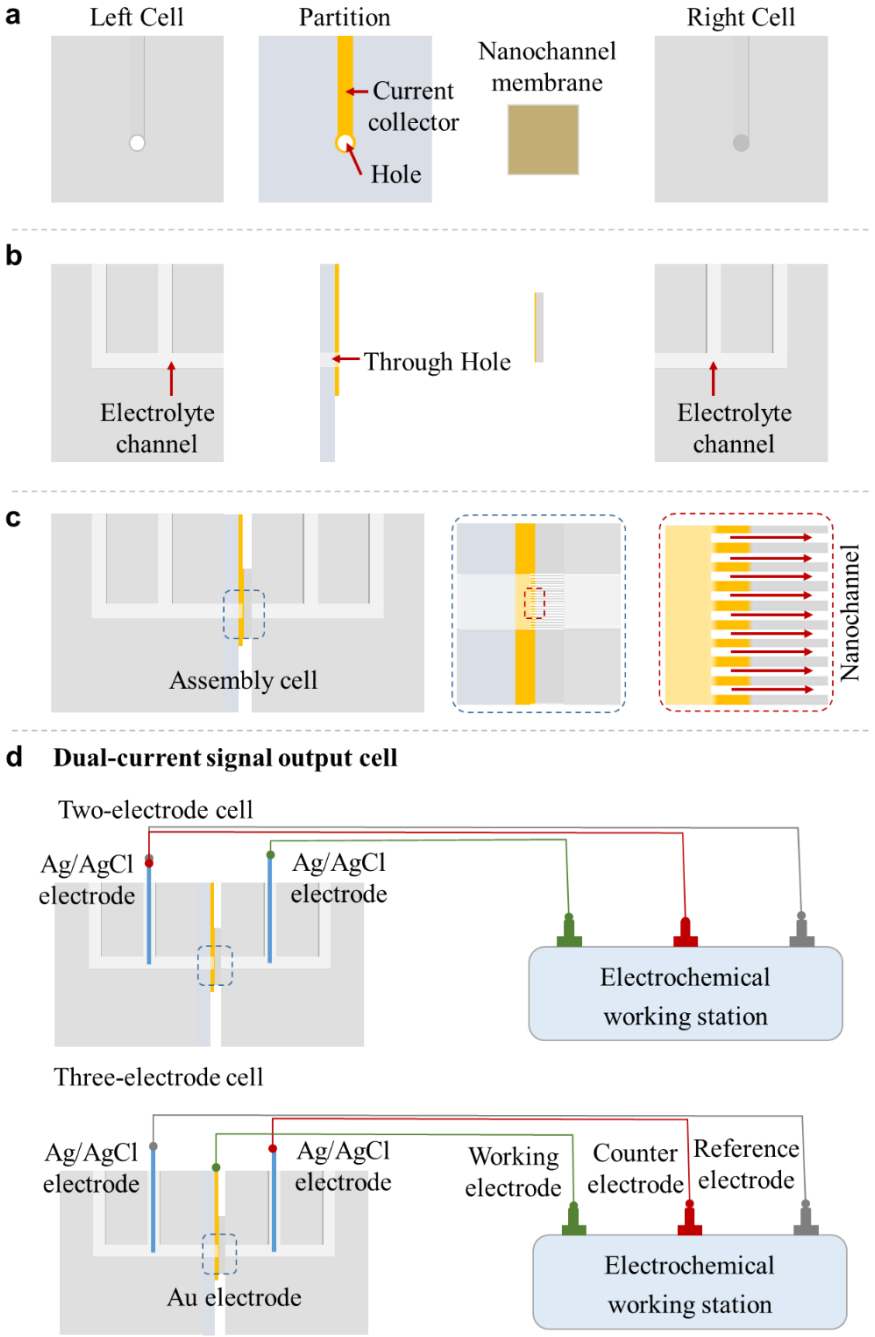

Supplementary Figure 6| a scheme of the three-electrode system, which contains the details about the working electrode connect and all the circuits. (a) scheme of components in three-electrode system from vertical view. (b) scheme of components in three-electrode system from sectional view. (c) scheme of assembled three-electrode system from sectional view. Enlarged view of joint between the nanochannels and the current collector. (d) a scheme of dual-current output cell. Setup of the two-electrode cell (top figure) and the three-electrode cell (bottom figure) connected with electrochemical working station.

Supplementary Figure 7

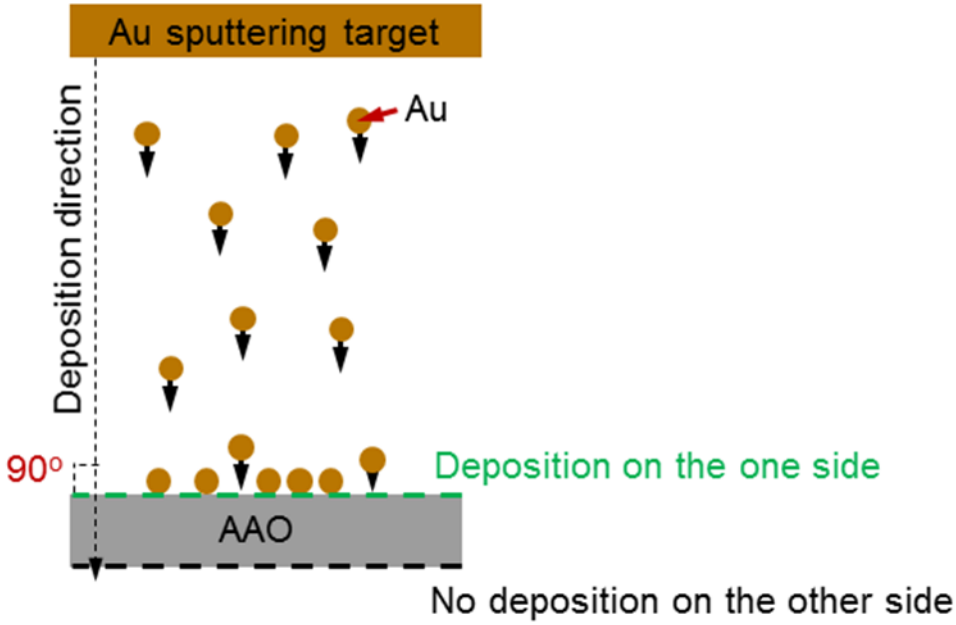

Supplementary Figure 7| Sketch map of metallic depositions. The Au (or ITO) deposition perpendicular to the outmost of AAO and at the one side of the AAO membrane's OS.

Supplementary Figure 8

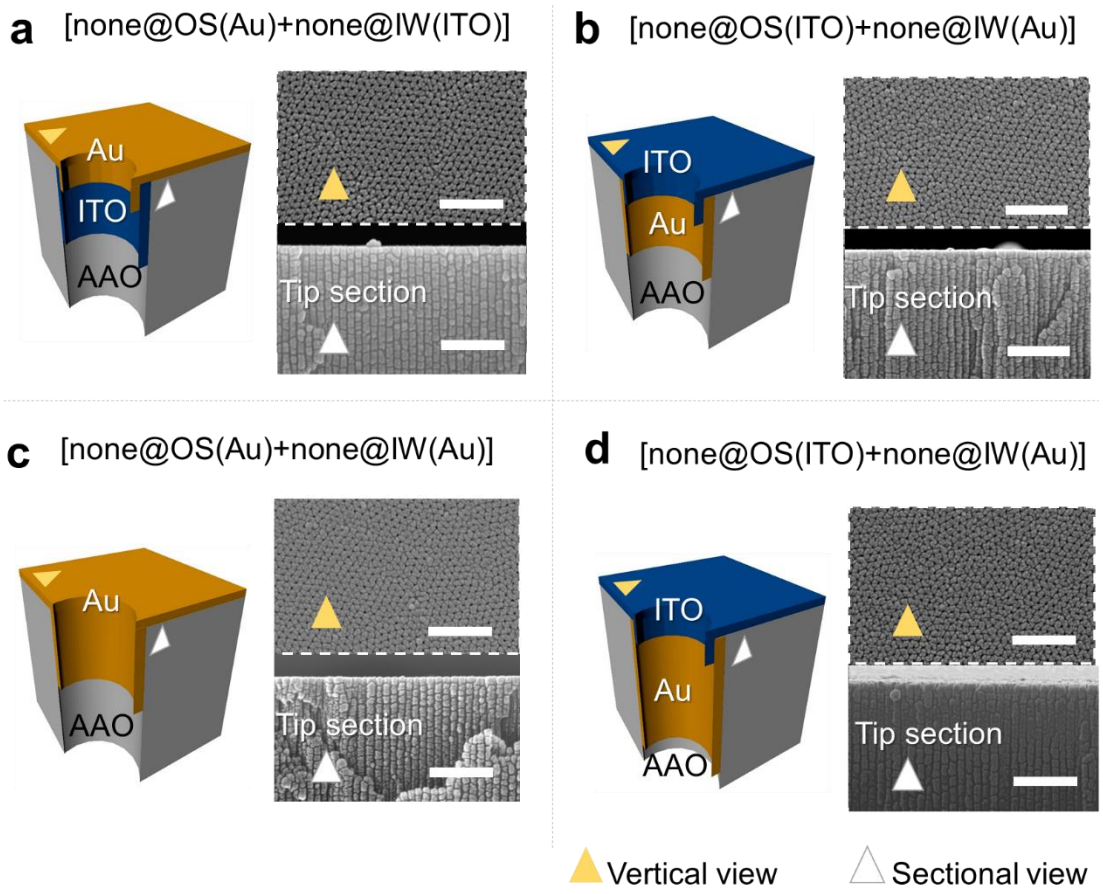

Supplementary Figure 8| SEM images of the four kinds of deposited nanochannels with different subsequent deposition, taken from vertical and sectional view. Reprinted with permission from ref. S2, Nature Press.

Supplementary Figure 9

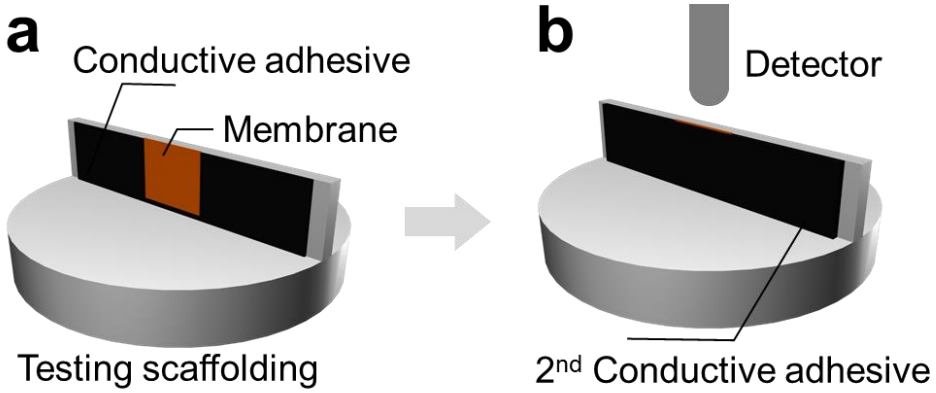

Supplementary Figure 9| Scheme of the setup for SEM or EDS detection.

Supplementary Figure 10

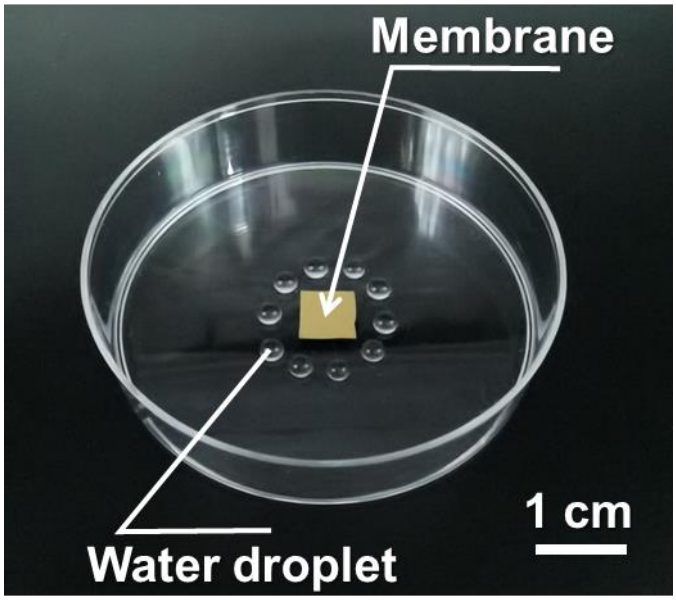

Supplementary Figure 10| Photograph of the membrane surrounded by water droplet for Steps 21.

Supplementary Figure 11

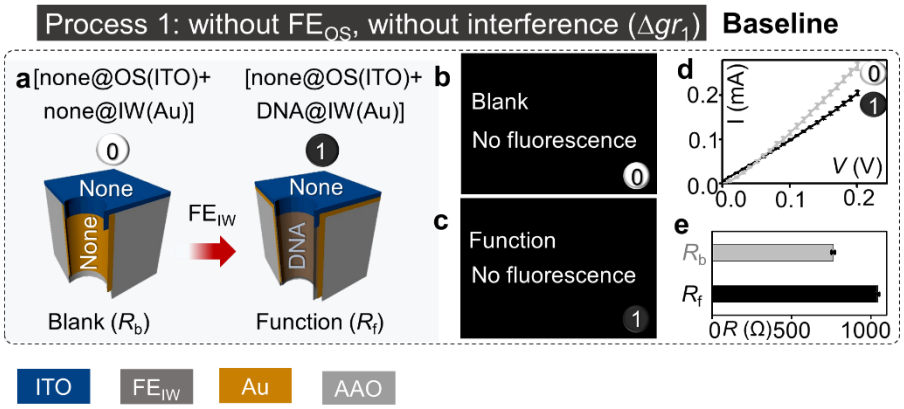

Supplementary Figure 11| The nanochannel without FEOS and without interference. (a) scheme of process 1 is from 0 state (without FEIW and interference) to 1 state (with FEIW but without interference). (b, c, d and e) four indexes were designed to evaluate the anti-interference ability of FEOS including fluorescent images (b), fluorescent intensity profiles (c), I-V curves (d) and resistances increment (e). Error bars represent standard deviations of three experimental replicates. Reprinted with permission from the Supplementary Figure 21 in ref. S2, Nature Press.

Supplementary Figure 12

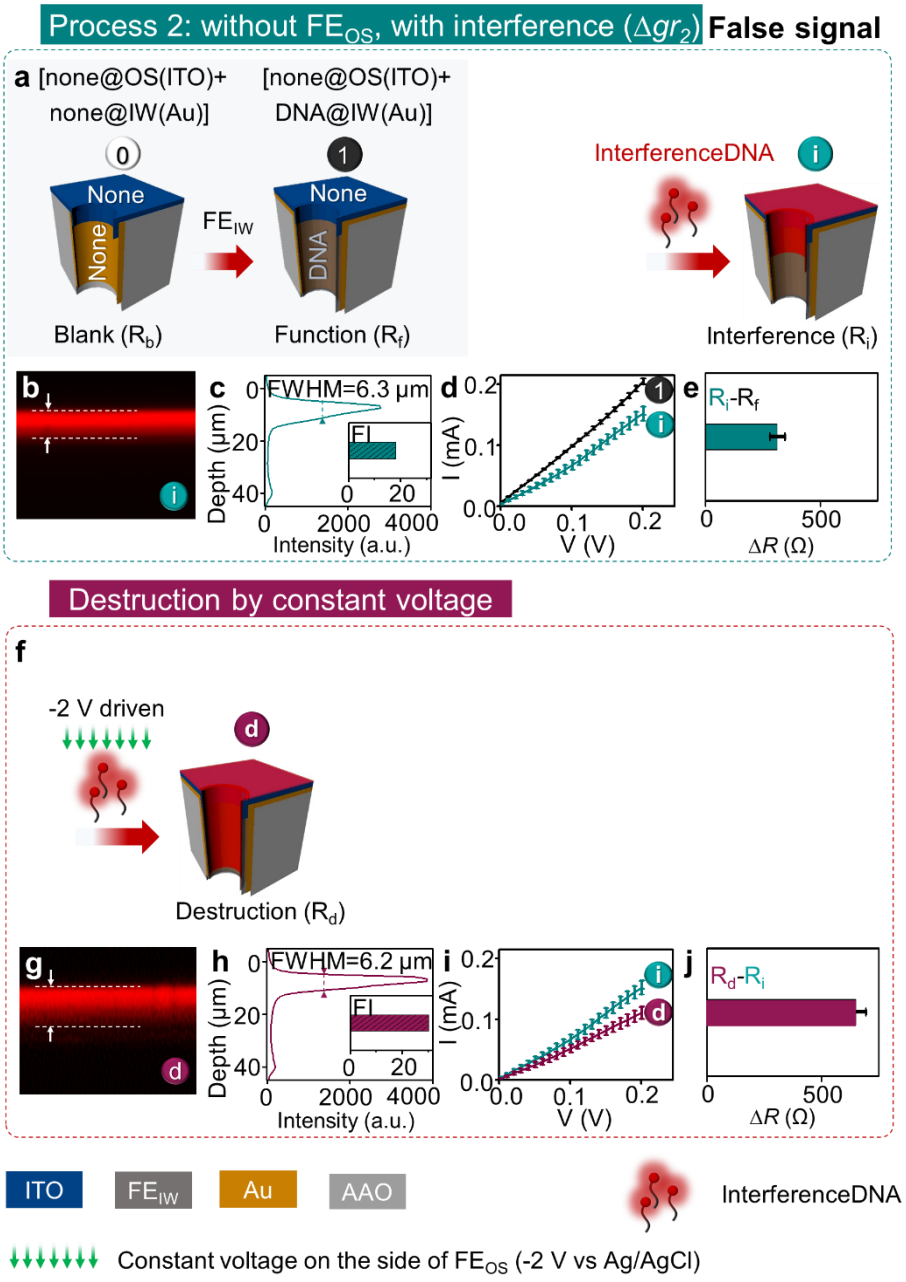

Supplementary Figure 12| The nanochannel without FEOS. Fluorescent-labelled DNA (InterferenceDNA) is used as interference molecules. (a and f) scheme of Process 2 is from 0 state to 1 state and then to i state (with FEIW and interference). Finally, the interference was driven into nanochannel under 2 V as d state. (b, c, d and e) four indexes were designed to evaluate the anti-interference ability of FEOS including fluorescent images (b), fluorescent intensity profiles (c), I-V curves (d) and resistances increment (e). Error bars represent standard deviations of three experimental replicates. Reprinted with permission from the Supplementary Figure 21 in ref. S2, Nature Press.

Supplementary Figure 13

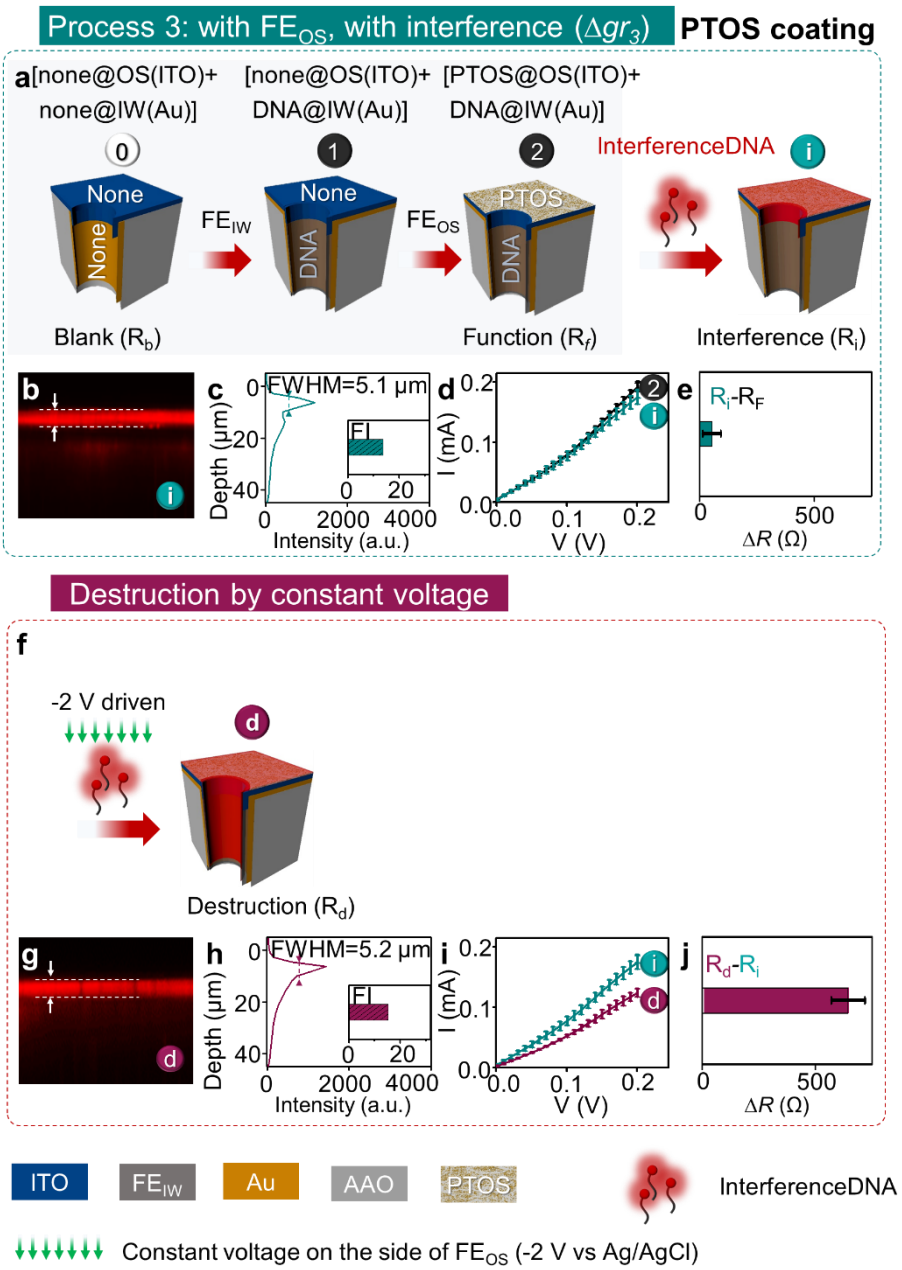

Supplementary Figure 13| The chosen hydrophobic molecules acting as FE$_{OS}$. Fluorescent-labelled DNA (InterferenceDNA) is used as interference molecules. (a and f) scheme of Process 3 is from 0 state to 1 state and then to state 2 with the chosen hydrophobic molecule acting as FE$_{OS}$, and i state (with FEIW and interference). Finally, the interference was driven into nanochannel under 2 V as d state. (b, c, d and e) four indexes were designed to evaluate the anti-interference ability of FE$_{OS}$ including fluorescent images (b), fluorescent intensity profiles (c), I-V curves (d) and resistances increment (e). Error bars represent standard deviations of three experimental replicates. Reprinted with permission from the Supplementary Figure 21 in ref. S2, Nature Press.

Supplementary Figure 14

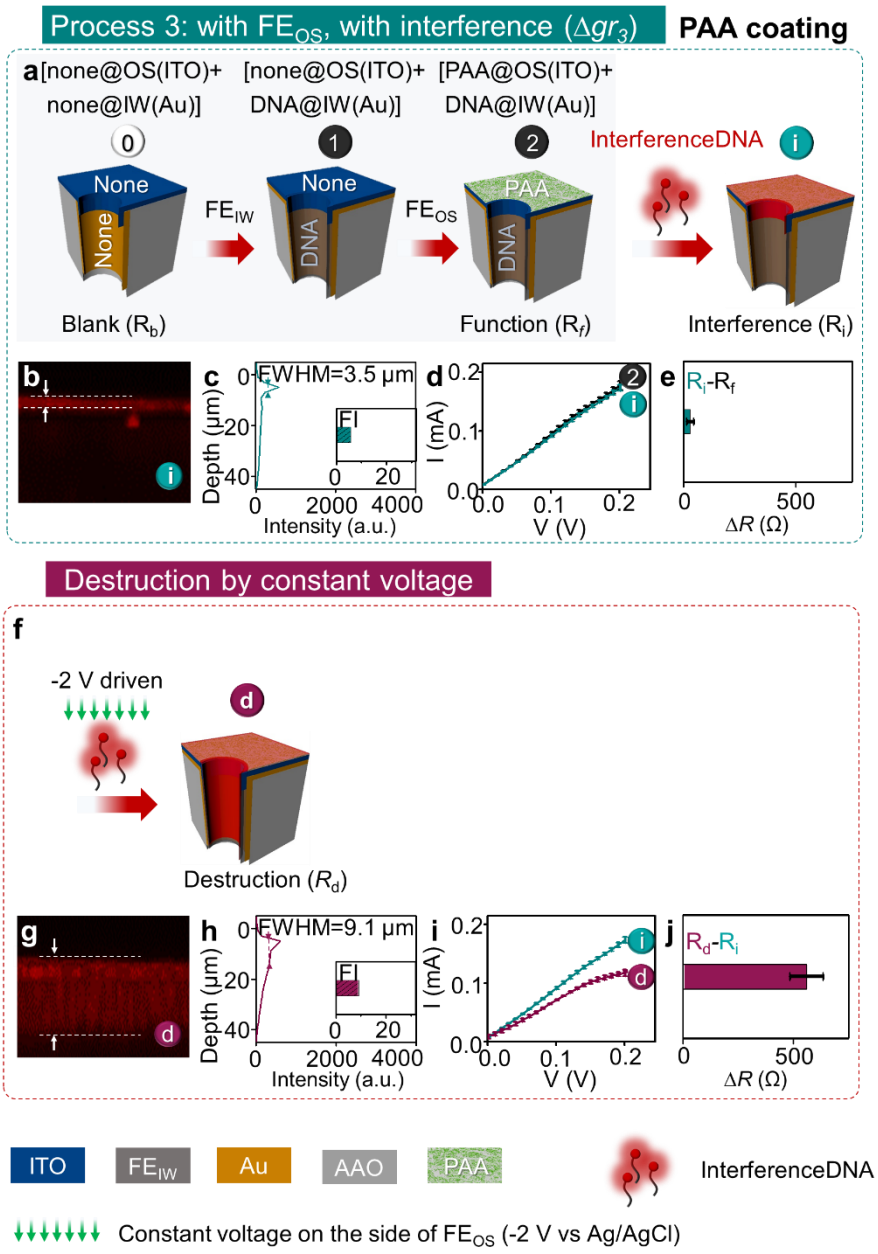

Supplementary Figure 14| The chosen negative charged molecules acting as FEOS. Fluorescent-labelled DNA (InterferenceDNA) is used as interference molecules. (a and f) scheme of Process 3 is from 0 state to 1 state and then to state 2 with the chosen negatively charged molecule acting as FEOS, and i state (with FEIW and interference). Finally, the interference was driven into nanochannel under 2 V as d state. (b, c, d and e) four indexes were designed to evaluate the anti-interference ability of FEOS including fluorescent images (b), fluorescent intensity profiles (c), I-V curves (d) and resistances increment (e). Error bars represent standard deviations of three experimental replicates. Reprinted with permission from the Supplementary Figure 21 in ref. S2, Nature Press.

Supplementary Figure 15

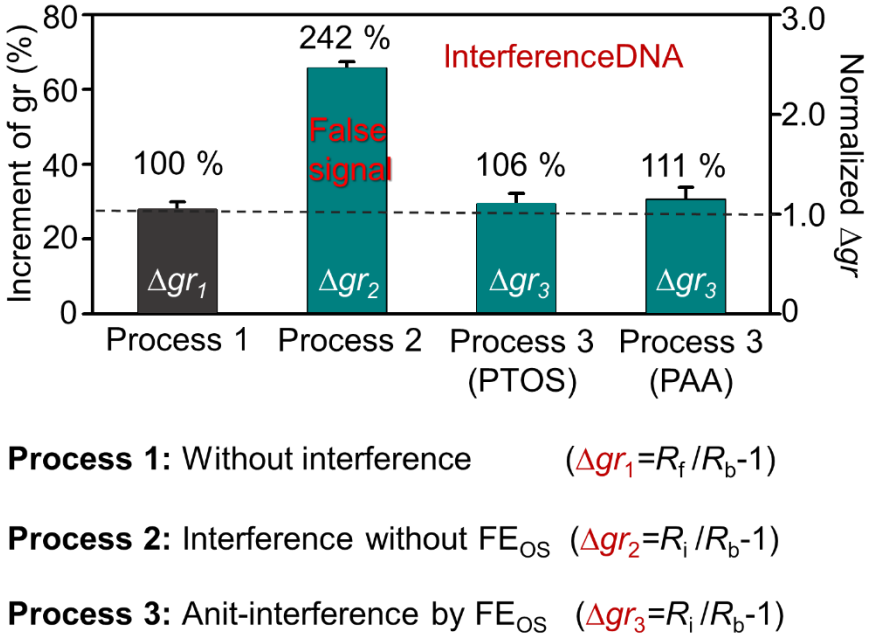

Process 1: Without interference ($\Delta gr_1=R_f/R_b-1$)

Process 2: Interference without FE_{OS} ($\Delta gr_2=R_i/R_b-1$)

Process 3: Anit-interference by FE_{OS} ($\Delta gr_3=R_i/R_b-1$)

Supplementary Figure 15| The chosen hydrophobic or negative molecules acting as FE_{OS}. Three different processes were designed to evaluate the anti-interference ability of FE_{OS}. Fluorescent-labelled DNA (InterferenceDNA) is used as interference molecules. The comparison and the definition of Δ*gr* during the three processes above.

Supplementary Figure 16

Gating systems	Gating Efficiency (%)		
Scheme	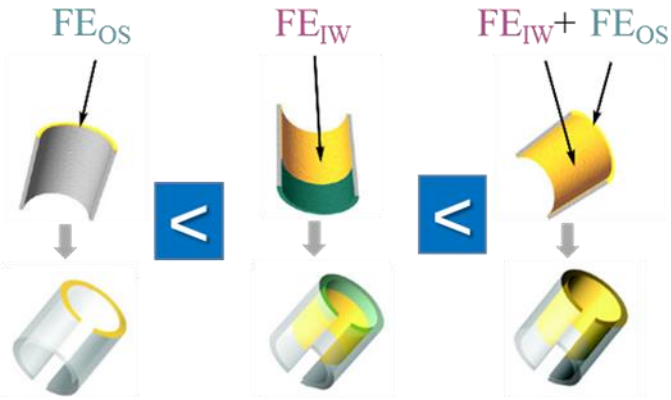		
Low-efficiency gating	12.6%	217%	248%
High-efficiency gating	9.4%	1356%	2285%

Supplementary Figure 16| Comparison of the efficiency of ion gating between nanochannels with regional functional elements using the hybrid complexes of probeDNA-SH and targetDNA (low-efficiency ion gating system) and supersandwich DNA complexes (high-efficiency ion gating system). Reprinted with permission from ref. S3, Nature Press.

Supplementary Table 1

Components of FE_{OS} and FE_{IW} factionalized nanochannels in Supplementary Figure 11-14. Reprinted with permission from ref. S2, Nature Press.

Specimen in Supplementary Figure 11-14	Element		Regional modified FEs	
	OS	IW	FEs@OS	FEs@IW
Supplementary Figure 11a(0)	ITO	Au	None	None
Supplementary Figure 11a(1)	ITO	Au	None	DNA
Supplementary Figure 12a(0)	ITO	Au	None	None
Supplementary Figure 12a(1)	ITO	Au	None	DNA
Supplementary Figure 13a(0)	ITO	Au	None	None
Supplementary Figure 13a(1)	ITO	Au	None	DNA
Supplementary Figure 14a(0)	ITO	Au	None	DNA
Supplementary Figure 14a(1)	ITO	Au	PAA	DNA

Reference

S1. Xu, X. et al. Coordination of the electrical and optical signals revealing nanochannels with an 'onion-like' gating mechanism and its sensing application NPG Asia Mater. 8, e234 (2016).

S2. Gao, P. et al. Distinct functional elements for outer-surface anti-interference and inner-wall ion gating of nanochannels. *Nat. Commun.* **9**, 4557 (2018).

S3. Li, X. et al. Role of outer surface probes for regulating ion gating of nanochannels. *Nat. Commun.* **9**, 40 (2018).